American Mineralogist, Volume 70, pages 88–105, 1985

Relationships between properties and structure of aluminosilicate melts

Bjørn O. Mysen, David Virgo and Friedrich A. Seifert[1]

Geophysical Laboratory, Carnegie Institution of Washington
Washington, D.C. 20008

Abstract

The structure of melts in the composition join $Na_2Si_2O_5$–$Na_4Al_2O_5$ has been evaluated by Raman spectroscopy of melts quenched at 1 atm from 1600°C, at 30 kbar quenched from 1600°C, and at 30 kbar quenched from 1400°C. The Al^{3+} is in tetrahedral coordination. Under all conditions, this tetrahedrally coordinated Al^{3+} displays strong preference for three-dimensional network units in the melts. The relative abundance of three-dimensional network units increases, therefore, with increasing Al/(Al+Si) of the melt even though its bulk NBO/T is unchanged (NBO/T, nonbridging oxygen per tetrahedrally coordinated cation). This increase is compensated for by an increase in the relative abundance of anionic units with NBO/T ≥ 2. The proportion of units with NBO/T = 1 decreases. These effects become more pronounced with increasing pressure at the same temperature.

For basaltic liquids with similar NBO/T and Al/(Al+Si) the type of charge-balancing cation for tetrahedrally coordinated Al^{3+} and the types of network-modifying metal cations control the relative importance of feldspar and olivine on the liquidus at 1 atm. Increasing $M^+/(M^+ + M^{2+})$ results in an increase in the relative abundance of three-dimensional aluminosilicate units and a decrease in SiO_4^{4-} units in the liquid. Thus, the liquidus volume of three-dimensional aluminosilicate minerals (feldspar) will increase as the alkali/alkaline earth increases. This trend is borne out by experimental phase-equilibrium measurements at 1 atm on natural rock compositions.

Introduction

Aluminum and silicon are the two most important network-forming cations in silicate melts. A systematic study of the structural role of aluminum in silicate melts is therefore necessary to the understanding of the structure of natural magmatic liquids.

Structure models of aluminosilicate melts represent an improvement over those deduced by extrapolation from data in simple binary metal oxide–silica systems. An example of the limitation of extrapolations of binary metal oxide–silicate melt structure data to aluminous melts is that such models (e.g., Mysen et al., 1982a) do not explain the large olivine liquidus field in many basaltic magmas (Kirkpatrick, 1983). Generally, binary metal oxide-silica melts with bulk melt NBO/T[2] ≤ 1 do not

[1] Present address: Mineralogisch-Petrographisches Institut und Museum, Universitat Kiel, Kiel, Federal Republic of Germany.

[2] NBO/T; nonbridging oxygens per tetrahedrally-coordinated cations. As shown, for example, by Mysen et al. (1982a), this ratio is a measure of degree of polymerization of a silicate melt and can be calculated from its bulk chemistry provided that (1) the types and proportions of tetrahedrally-coordinated cations are known and that (2) "free" oxygens (in the sense of Toop and Samis, 1962) do not exist. Free oxygen (O^{2-}) has been documented only in melts that are less polymerized than that of pyrosilicate (see data and discussion in Bottinga et al., 1981; and Mysen et al., 1982a, and references therein). Even if calculated with the unrealistic assumption that only Si^{4+} is in tetrahedral coordination in naturally-occurring magmatic liquids, these liquids are more polymerized than that of metasilicate. Thus, free oxygens are extremely unlikely, and the oxygen budget can be described in terms of only bridging (BO) and nonbridging (NBO) oxygens. In order to assign the tetrahedrally-coordinated cations (T-cations), structural information is required. In addition to Si^{4+}, the most likely T-cations in silicate melts compositionally relevant to natural magmatic liquids are Al^{3+}, P^{5+}, Ti^{4+} and Fe^{3+}. All available structural data show that provided that there are sufficient M^+ and M^{2+} metal cations available for charge-balance, Al^{3+} is in tetrahedral coordination, at least at 1 atm pressure (e.g., Taylor and Brown, 1979a,b; McMillan and Piriou, 1983; McMillan et al., 1982; Navrotsky et al., 1982; Mysen et al., 1981a; Seifert et al., 1982a). Both P^{5+} and Ti^{4+} are T-cations in melts as indicated by both structural and liquidus phase equilibrium information (Kushiro, 1975; Ryerson and Hess, 1980; Visser and Koster van Groos, 1979; Mysen et al., 1980b, 1981b, 1982a). Ferric iron commonly is in tetrahedral coordination with the same charge-balance constraints as for Al^{3+} (e.g., Fox et al., 1982; Virgo et al., 1982, 1983; Mysen and Virgo, 1983; Mysen et al., 1984) with possible limitations imposed by low $Fe^{3+}/\sum Fe$ (Virgo et al., 1983; Mysen et al., 1984).

Detailed structural considerations such as those summarized above enter into the calculation of NBO/T. Given these pre-

0003–004X/85/0102–0088$02.00

contain significant amounts of orthosilicate units. Basaltic melts with similar bulk melt NBO/T apparently do contain orthosilicate units, in view of the fact that olivine commonly precipitates on their liquidus at 1 atm (Kirkpatrick, 1983). A similar conclusion may be drawn from the "quasi-crystalline" model of silicate melts proposed by Burnham (1974, 1981). It may be suggested that the expanded olivine liquidus field observed in natural basaltic liquids is related to the role of aluminum in the structure of these more complex silicate melts.

It has been shown that density, compressibility and viscosity of silicate melts depend strongly on their degree of polymerization (Shartsis et al., 1952; Bockris et al., 1955; Bockris and Kojonen, 1960; Rontgen et al., 1960; MacKenzie, 1960; Gaskell, 1982). These melt properties are particularly sensitive to M/Si (or NBO/Si) in the compositional range (<33 mole % metal oxide) where three-dimensional network units occur in the melt (Mysen et al., 1982a). The $Al^{3+} \rightleftharpoons Si^{4+}$ substitution in fully polymerized (NBO/T = 0) aluminosilicate melts results in a rapid decrease in the melt viscosity and activation energy of viscous flow as the bulk melt Al/(Al+Si) increases (Riebling, 1966). The values of these two properties are significantly less dependent on Al/(Al+Si) the greater the Na/Al of the melts (see Riebling, 1966; Bockris et al., 1955). Moreover, these same two physical properties become increasingly sensitive to pressure changes with increasing Al/(Al+Si) in aluminosilicate melts with three-dimensionally interconnected structure (Kushiro, 1980). In depolymerized aluminosilicate melts, aluminum may exhibit a preference for specific structural units (Mysen et al., 1981a) so that the Al/(Al+Si) in the units differ from each other. Such a structural configuration is likely to affect the rheological behavior of the melts. Furthermore, this suggested distribution of Al^{3+} between the structural units is likely to be pressure, temperature and bulk composition dependent. It is therefore fundamentally important to evaluate the role of Al^{3+} in silicate melts whose structures resemble those of magmatic liquids in order to understand the pressure, temperature and compositional dependence of these melt properties.

mises, one may calculate bulk melt NBO/T from the expressions (Mysen et al., 1982a, 1984):

$$\mathrm{NBO/T} = (4 \times \mathrm{T} - 2 \times \mathrm{O})/\mathrm{T} = \sum_{i=1}^{i} \mathrm{n}M_i^{n+}/\mathrm{T},$$

where M^{n+} represent network-modifying cations. Their sum is obtained after subtraction of the proportion of metal cations necessary for charge-balance of Al^{3+} and Fe^{3+}.

Thus, with these considerations in mind the bulk melt NBO/T can be used as a compositional and structural indicator of silicate melts. In this report, NBO/T denotes bulk melt nonbridging oxygen per tetrahedral cation. The nbo/t is used to express the nonbridging oxygens per tetrahedral cations in individual structural units.

The present study was undertaken to isolate the influence of Al/(Al+Si) on the melt structure in melts with NBO/T >0. Experiments were also conducted at various temperatures and pressures in order to study the structure of silicate melts under conditions relevant to magmatic processes in the earth and terrestrial planets.

Starting compositions

All compositions were in the system Na_2O–Al_2O_3–SiO_2 (Fig. 1) along the composition join sodium disilicate (NS2)-sodium dialuminate (NA2). With Al^{3+} in tetrahedral coordination these melts have bulk NBO/T = 1. This degree of polymerization was chosen because of its similarity to that of basaltic liquids (see Mysen et al., 1982a, for calculations). Furthermore, aluminum-free sodium disilicate melt contains only a small proportion (<20%; Mysen et al., 1982a; Furukawa et al., 1981) of three-dimensionally interconnected structural units and only a low relative abundance of units with nbo/si >1 (<20%). As a result, possible changes in their relative abundance with increasing Al/(Al+Si) of the melt may be easily detected. Finally, the phase relations along the composition join chosen here (Fig. 1) show that liquidus minerals change from sodium disilicate (NBO/Si = 1) to sodium metasilicate (NBO/Si = 2) and finally to carnegieite (NBO/T = 0) with increasing bulk melt Al/(Al+Si)

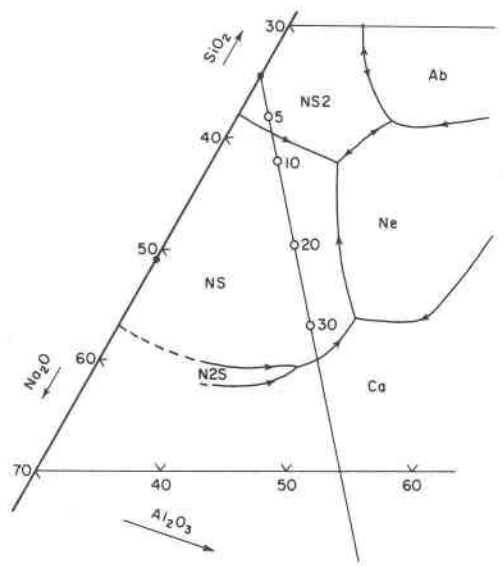

Fig. 1. Compositions of starting materials with simplified liquidus phase relations in the system Na_2O–Al_2O_3–SiO_2 (wt.%) (Osborn and Muan, 1960a). Symbols: NS2, $Na_2Si_2O_5$; N2S, Na_4SiO_4; Ca, carnegieite ($NaAlSiO_4$); Ne, nepheline ($NaAlSiO_4$); NS, $NaSiO_3$; Ab, albite ($NaAlSi_3O_8$). The line with open circles is a portion of the composition join $Na_2Si_2O_5$–$Na_4Al_2O_5$. Numbers along the line reflect compositions (mole % $Na_4Al_2O_5$ component replacing $Na_2Si_2O_5$ component) of starting materials.

(see also Osborn and Muan, 1960a). Thus, inasmuch as liquidus phase equilibria reflect the structural properties (and, thus thermodynamic properties) of both the melts and coexisting mineral(s), the liquidus equilibria in this portion of the system Na_2O–Al_2O_3–SiO_2 may provide a clue as to how the aluminum abundance may affect the stability of depolymerized silicate minerals (e.g., meta- and orthosilicate) on the liquidus of basalt.

Experimental methods

Sodium-bearing silicate melts tend to lose Na by volatilization at high temperatures in open sample containers. This experimental complication becomes increasingly severe with increasing Na content of the liquid (Kracek, 1930; Seifert et al., 1979a; Bigger, 1981). The problem is compounded by the fact that glasses with high sodium content [in the present study, Na_2O increases from about 34 wt.% in $Na_2Si_2O_5$ to about 42 wt.% in NS2(NA2)30 (70 mole % sodium disilicate component and 30 mole % sodium dialuminate)] are not amenable to electron microprobe analysis because of the volatile nature of Na under the electron beam. In order to document the nominal melt compositions, Seifert et al. (1979a) used combinations of crystallization experiments of NS2 with subsequent optical and X-ray studies, and Raman spectroscopy of quenched silicate melts on the join Na_2O–SiO_2 as a function of intensive and extensive variables, to determine the composition of the starting materials. Because melts on the join $Na_2Si_2O_5$–$Na_4Al_2O_5$ do not crystallize to a phase of the same composition and the spectroscopic data *a priori* cannot be used to determine whether the nominal composition has been affected by the preparation technique, the melts studied here cannot be subjected to the same tests as those on the binary join Na_2O–SiO_2. In view of the fact that the liquidus temperatures and sodium contents are comparable to those on the analogous Al-free Na_2O–SiO_2 join (Osborn and Muan, 1960a), the same methods of preparation found to be satisfactory by Seifert et al. (1979a) were employed here.

The starting glasses were formed by initial decarbonation of Na_2CO_3 in finely ground (~1 μm) mixtures together with spectroscopically pure SiO_2 and Al_2O_3 at 800°C for 24 hr. The temperature was then raised slowly to 1000°C and kept there for 1 hr to melt the compositions. Batches of approximately 250 mg of starting material were prepared in this manner.

Experiments at 1 atm and 1600°C were conducted in a $MoSi_2$-heated, vertical quench furnace. The samples were contained in sealed Pt capsules of 3-mm diameter (1 cm long) in order to avoid Na loss at these high temperatures (~600°C above the liquidus). Run durations were 10–15 min. The experimental charges were quenched in liquid nitrogen at the rate of about 500°C/sec.

High-pressure experiments were carried out in solid-media, high-pressure apparatus (Boyd and England, 1960) with 1/2-in.-diameter furnace assemblies and sealed, 3-mm-o.d. Pt capsules. The experiments were terminated by turning off the power to the furnace. The quenching rate was about 250°C/sec. The samples were held at the same pressure by increasing the hydraulic pressure on the piston during temperature quenching in order to maintain pressure in the 1–2 sec period during which the liquids remained above their liquidus temperatures after the electrical power was turned off. Otherwise, a pressure drop of approximately 15%, during which the experimental charges remained in the superliquidus region, would be experienced.

Raman spectra were obtained with the automated Raman system described by Mysen et al. (1982b) and Seifert et al. (1982a). Approximately 1-mm^3 chips of glass were excited with a Coherent CR-18 Ar^+-ion laser operating at 2–4 W. Other details of the Raman procedure, data acquisition and storage and deconvolution of the spectra were identical with those reported by Seifert et al. (1982a) and Mysen et al. (1982b). Interested readers are referred to those papers for discussion of choice of line shapes, number of lines, statistical limitations and tests of the quality of the fits of the deconvoluted spectra as well as relevant aspects of the computer programs used.

Effect of quenching

The data reported here as well as most other structural data on silicate melts have been obtained on quenched melts (glass). It is therefore necessary to assess the extent to which quenching may have affected the structure of the material. Data on glasses and equivalent melts obtained at 1 atm in the system Na_2O–Al_2O_3–SiO_2 (Sweet and White, 1969; Sharma et al., 1978a; Seifert et al., 1981a) indicate that with the quenching rates attainable in vertical quench furnaces similar to that used here, there is no spectroscopic evidence, within the sensitivity of the methods, for structural differences between a glass and its 1-atm molten equivalent. This conclusion is not meant to imply, however, that differences in heat capacity, for example, of materials above and below their glass transition points (e.g., Navrotsky et al., 1980) are not due to variations in melt structure. It is only suggested that the features discernible with the available analytical tools do not reflect changes that may have occurred during cooling through the glass transition point.

No comparable data are available for glasses quenched at high pressure. It is likely that any pressure-induced structural change would involve a decrease in volume and that the dT/dP for such transformations are probably positive (in analogy with possible analogous transformations in crystalline aluminosilicate systems). As a result, isobaric temperature quenching of possible pressure-induced structural changes in the melts is unlikely to result in a back reaction to a structure that is stable at lower pressure. In fact, isobaric temperature quenching of possible transformations with positive dT/dP shifts the sample farther away from the pressure and temperature conditions under which the transformation(s) may have occurred.

Experimental results

Raman spectra of quenched melts on the composition join $Na_2Si_2O_5$–$Na_4Al_2O_5$ as a function of Al/(Al+Si), temperature and pressure are shown in Figures 2–4. The spectra of quenched sodium disilicate melts at all pressures and temperatures are similar to each other and to those reported by others for the same composition (Brawer and White, 1975; Verweij, 1979b). The high-frequency envelope (800–1200 cm^{-1}) consists of three polarized (900-, 950- and 1100-cm^{-1}) and two depolarized (1070- and 1150-cm^{-1}) bands. In addition, there is an asymmetric, polarized band near 620 cm^{-1} and a very weak, broad band near 780 cm^{-1}. Substitution of 5 mole % NA2 ($Na_4Al_2O_5$) component for NS2 [to produce bulk composition NS2(NA2)5] results in a shift of the 1070-cm^{-1} band to 1050–1060 cm^{-1} coupled with an increase in its relative intensity (Figs. 2–4; Table 1). This band may be

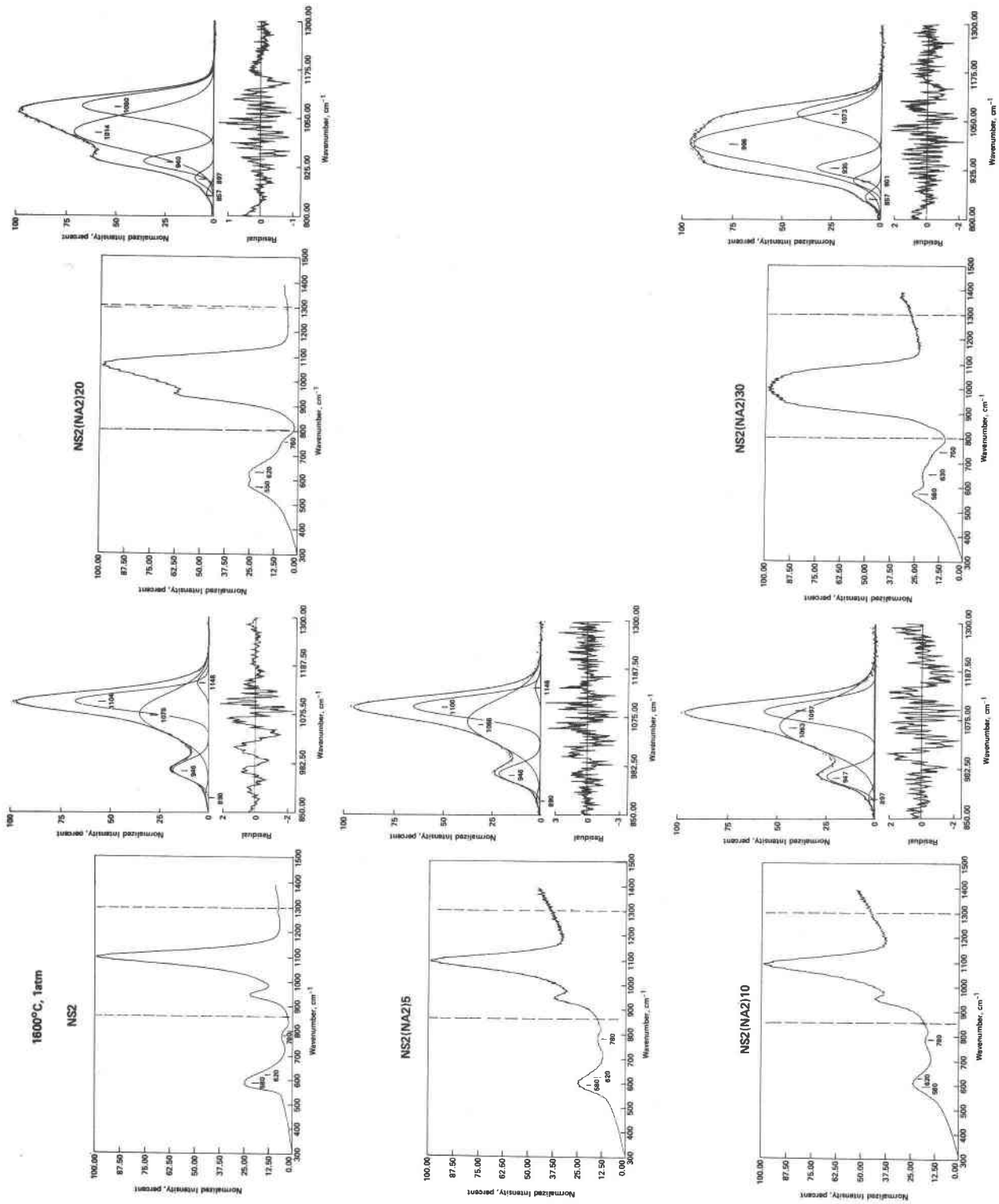

Fig. 2. Unpolarized, frequency and temperature-normalized (see Mysen et al., 1982b) Raman spectra of melts on the join NS2-NA2 at 1 atm quenched from 1600°C. Composition symbols NS2(NA2)5, etc., denote mole % NA2 component ($Na_4Al_2O_5$) replacing NS2 component ($Na_2Si_2O_5$).

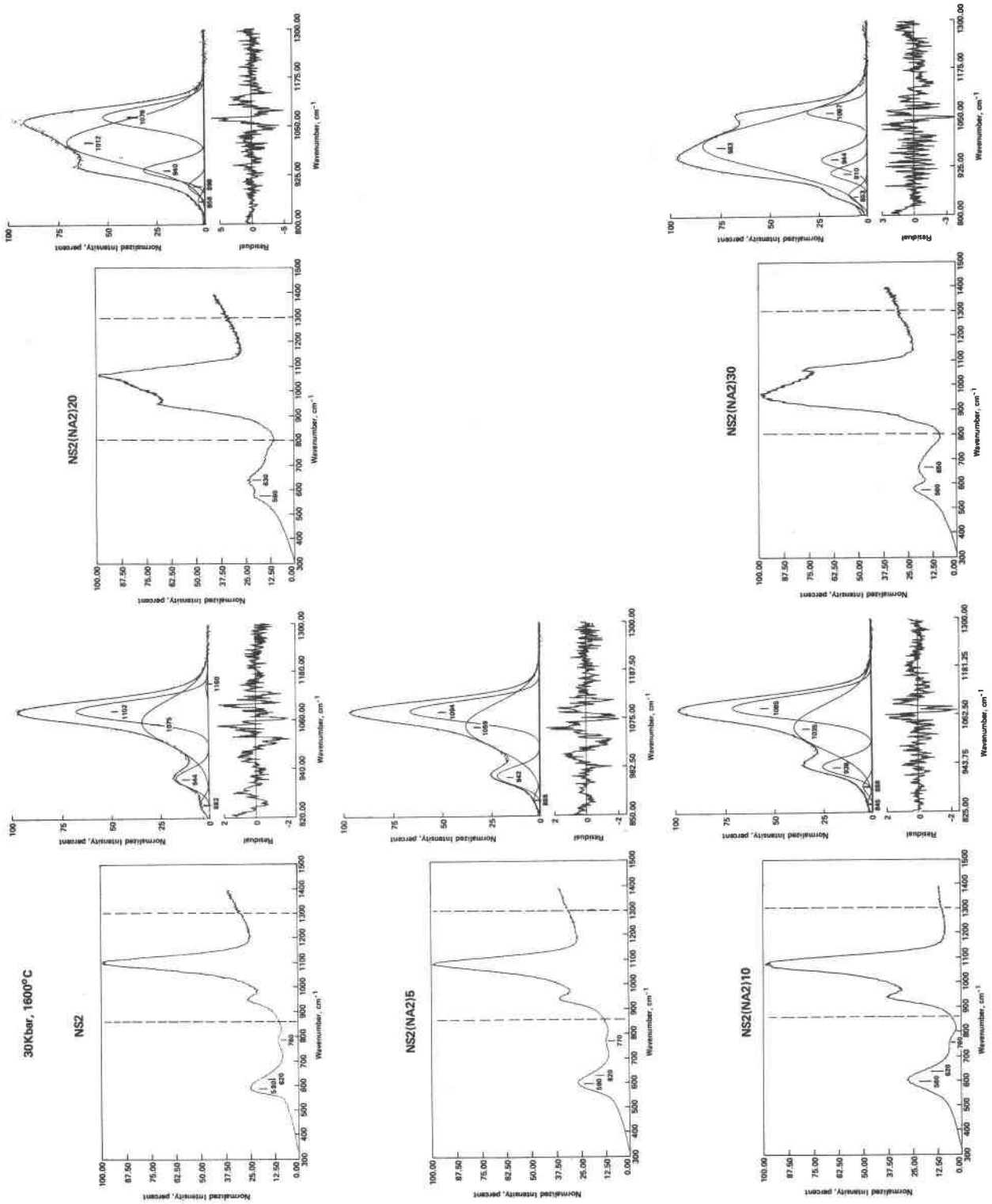

Fig. 3. Same as Fig. 2 but at 30 kbar quenched from 1600°C.

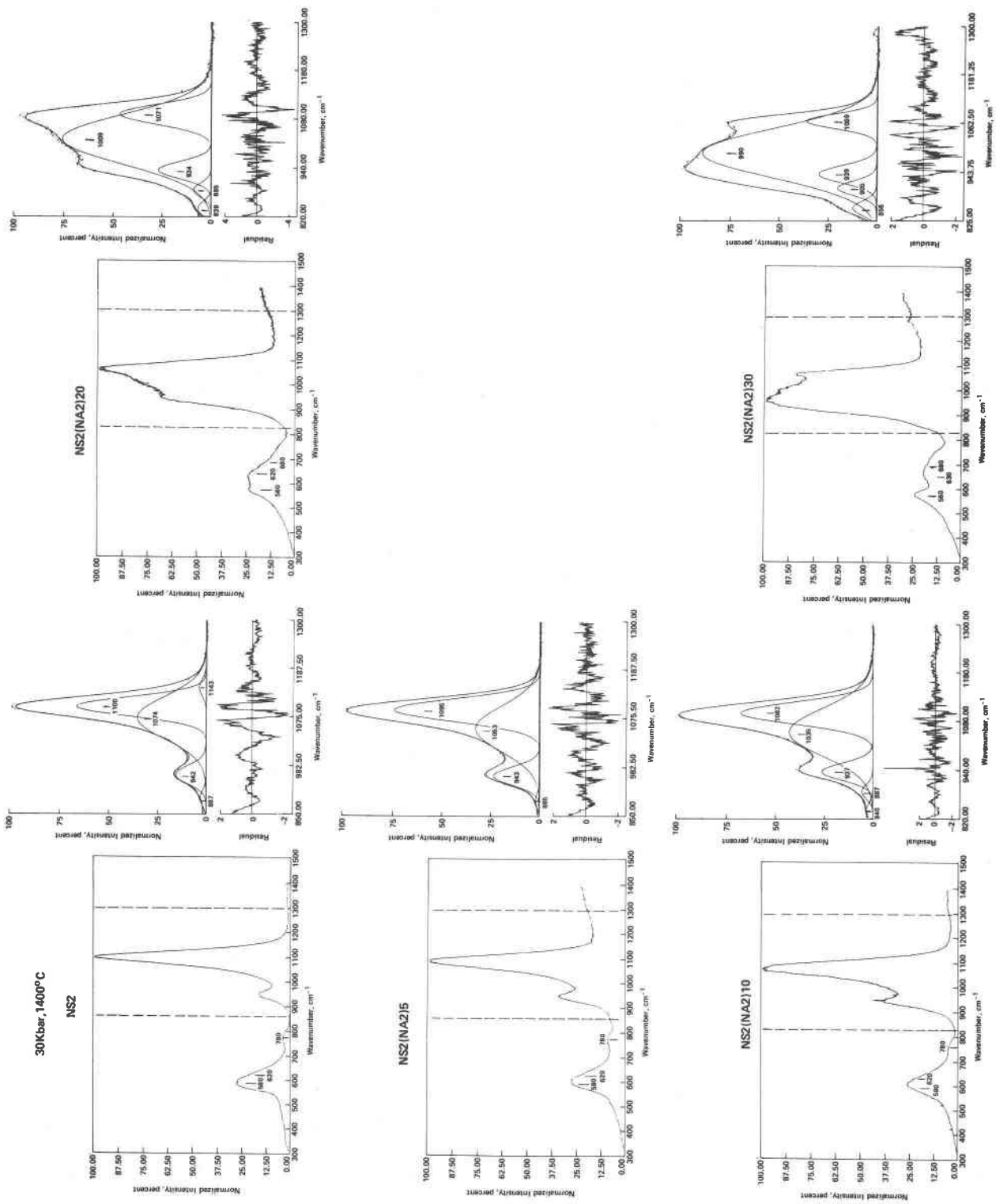

Fig. 4. Same as Fig. 2 but at 30 kbar quenched from 1400°C.

Table 1. Relative intensities (%) of Raman bands in the high-frequency envelope between 850 and 1200 cm^{-1}

Mole % NA2	1050/ΣArea	1100/Area(1)	950/Area(1)	900/Area(1)	860/Area(1)
		0.001 kbar, 1600°C			
0	44.7	78.4	20.2	1.4	-
5	47.4	76.8	21.9	1.4	-
10	56.5	70.4	26.8	2.8	-
20	59.2	67.6	24.9	5.6	2.0
30	68.5	53.6	29.8	10.6	6.0
		30 kbar, 1600°C			
0	45.7	78.8	17.2	3.9	-
5	48.1	75.3	22.1	2.6	-
10	45.7	74.8	20.3	3.2	1.7
20	62.2	62.3	28.6	6.3	2.8
30	77.2	36.3	32.0	21.2	10.5
		30 kbar, 1400°C			
0	47.6	79.2	18.0	2.8	-
5	41.2	78.2	20.3	1.6	-
10	49.7	72.0	21.8	3.8	2.4
20	69.5	57.3	28.7	8.0	6.1
30	74.2	35.1	34.2	19.1	11.6

ΣArea: Sum of relative intensites of 860-, 900-, 950-, 1050-, 1100- and 1150-cm^{-1} bands.

Area(1): Sum of relative intensities of 860-, 900-, 950- and 1100-cm^{-1} bands. The 1050-cm^{-1} band represents that between about 1000 and 1070 cm^{-1}, depending on Al/(Al + Si).

Calculated scattering efficiency factors (see text): $Si_2O_5^{2-}$, 1.0; SiO_3^{2-}, 0.5; $Si_2O_7^{6-}$, 0.33; SiO_4^{4-}, 0.3 (estimated).

deconvoluted into two bands (near 1000 cm^{-1} and 1070 cm^{-1}) for NS2(NA2)5 composition, whereas for higher Al content the statistical deconvolution procedure (Mysen et al., 1982b) results in a merger of the two bands unless one or more line parameters (frequency, half-width or intensity) are constrained (held constant) during the fitting procedure. There is no *a priori* information with which to justify such constraints, and deconvolution of this spectral region with constraints on the line parameters was not continued.

The spectrum of quenched NS2(NA2)10 melt (10 mole % sodium dialuminate component) at 1 atm represents a further evolution of the NS2 and NS2(NA2)5 spectra (Fig. 2). For the spectra quenched from 1600° and 1400°C at 30 kbar (Figs. 3 and 4), there is a small difference, in that the 1100-cm^{-1} band is shifted to about 1080 cm^{-1}, the 1150-cm^{-1} band can no longer be discerned and both a 900- and an 860-cm^{-1} band are present. Additional aluminum results in a further slow decrease in the frequency of the 1100-cm^{-1} band, a more rapid decrease in the frequency of the band between 1070 and 1000 cm^{-1}, a rapid increase in the relative intensity of the band at 1000-1070 cm^{-1} and an increase in the intensities of the 860-, 900- and 950-cm^{-1} bands relative to that of the 1100-cm^{-1} band (Table 1). The band or group of bands near 600 cm^{-1} shows an initial increase in the frequency of its center of gravity and a decrease in intensity relative to the high-frequency envelope. With 20 mole % or more NA2 component, a new band appears near 550–560 cm^{-1} (Figs. 2–4).

Interpretation of spectra

The spectra shown in Figures 2–4 may be interpreted on the basis of the spectroscopic features of binary metal oxide–silica melts and those of silicate melts on aluminate-silica joins. For Al^{3+} it must also be established whether or not aluminum is in tetrahedral coordination in the pressure and temperature range under consideration. If Al^{3+} is tetrahedrally coordinated, it is important to determine whether it is substituted randomly for Si^{4+} in the melt or whether Al^{3+} may exhibit a preference for particular anionic units.

Sodium disilicate glass

Before the role of Al^{3+} is addressed, a brief summary of the salient points in the interpretation of the spectrum of quenched NS2 melt is necessary. The 900-, 945- and 1100-cm^{-1} bands (Figs. 2–4) are assigned to symmetric Si–O^- stretching (O^- denotes nonbridging oxygen) in anionic units with nonbridging oxygens per silicon (nbo/si) about 3, 2 and 1, respectively (e.g., Lazarev, 1972; Verweij, 1979a,b; Furukawa et al., 1981; McMillan et al., 1982; Domine and Periou, 1983; McMillan and Piriou, 1983; Virgo et al., 1980; Mysen et al., 1982a). In units with nbo/si = 4, the symmetric Si–O^- stretch band is near 860 cm^{-1} (Verweij and Konijnendijk, 1976; Furukawa et al., 1981; Gibbs et al., 1981; McMillan and Piriou, 1983). The asymmetric band or group of bands near 600 cm^{-1} has been assigned to a mixed bending and stretching vibration of the Si–O–Si group. The frequency of this band increases as the Si–O–Si angle increases (Furukawa et al., 1981). This interpretation is consistent with its position near 580–600 cm^{-1} in $Si_2O_5^{2-}$ groups, near 620–640 cm^{-1} in SiO_3^{2-} groups and near 700 cm^{-1} in $Si_2O_7^{6-}$ groups. The asymmetry of this band in quenched NS2 melt might thus be due to the coexistence of more than one anionic unit in the melt. The sodium disilicate quenched melt appears to consist, therefore, primarily of coexisting $Si_2O_5^{2-}$ and SiO_3^{2-} units with a minor contribution from $Si_2O_7^{6-}$ and SiO_2 units, where the relative abundance is $Si_2O_5^{2-} > SiO_3^{2-} > SiO_2 > Si_2O_7^{6-}$ (see also Fig. 10, Mysen et al., 1982a).

Network-modifying aluminum

It is commonly concluded that Al^{3+} is in tetrahedral coordination in aluminum silicate melts with sufficient M^+ or M^{2+} cations for charge-balance at least at 1 atm pressure. Only a brief discussion of possible spectroscopic consequences of network-modifying Al^{3+} is therefore necessary. Coordination transformation of Al^{3+} from a network former to a network modifier in a melt with

$T_2O_5^{2-}$ ($T = Al^{3+} + Si^{4+}$) stoichiometry may be expressed with the formalized equation:

$$5Si_2O_5^{2-} + (NaAl)_2O_5^{2-} = 10SiO_3^{2-} + 2Na^+ + 2Al^{3+}(VI). \quad (1)$$

Expressions similar to equation 1 may be written to include other anionic units. Regardless of which expression is chosen, a coordination transformation of Al^{3+} in any of the compositions will cause a rapid increase in the relative intensities of Raman bands that result from Si–O^- stretch vibrations. The calculated value of NBO/T of all the starting compositions with Al^{3+} assumed to be in six-fold coordination [Al^{3+}(VI)] is shown in Table 2. For melts on the join Na_2O–SiO_2, increasing NBO/Si from that of sodium disilicate (NBO/Si = 1) results in a rapid increase in the abundance of SiO_3^{2-} units (see Fig. 6, Furukawa et al., 1981; and Fig. 10, Mysen et al., 1982a) and a slower increase in relative abundance of $Si_2O_7^{6-}$ and SiO_4^{4-} units (Mysen et al., 1982a). The units with nbo/si about 1 or 0, respectively, disappear quickly. For a direct comparison with the Raman spectra in Figure 4 in Mysen et al. (1982a), approximately 12 mole % NA2 component with aluminum as Al^{3+}(VI) results in bulk melt NBO/Si similar to that of composition Na_2O $1.2SiO_2$ (NBO/Si = 1.7). It is evident from the spectra in Figures 2–4 and a comparison with the spectra of melts on the join Na_2O–SiO_2 (see Fig. 4 in Mysen et al., 1982a) that increasing Al/(Al+Si) or increasing pressure and decreasing temperature do not result in an evolution of the Raman spectra comparable to that expected if Al^{3+} were a network modifier (rapid increase near 950 cm^{-1} and a slower increase between 860 and 900 cm^{-1}). Instead, there is a rapid intensity increase in the region between 1000 and 1050 cm^{-1} with the intensities of all the other stretch bands decreasing relative to this band (Table 1). Thus, there is no spectroscopic evidence for octahedrally coordinated aluminum in these quenched melts under any of the conditions studied.

Aluminum in tetrahedral coordination

In order to establish the location of tetrahedrally coordinated Al^{3+} in more detail, it is necessary to evaluate the various possible mechanisms of Al ⇌ Si substitution in relation to the interpretation of the Raman spectra. This discussion is best conducted with data on aluminate-silicate melts where it is established that Al^{3+} is tetrahedrally coordinated in three-dimensionally interconnected structures. Two fundamentally different spectroscopic interpretations of the Raman spectra of such glasses have been presented. McMillan et al. (1982) (see also McMillan and Piriou, 1983, and Piriou and Alain, 1979) suggested (p. 2031) that the the Si–O bond in Si–O–Al bridges can be spectroscopically treated as "Si–O stretching motions modified by Al^{3+} as a cation coordinating the oxygen, similar to alkali and alkaline earth cations in simple binary silicate glasses (e.g., Brawer and White, 1975)." Thus, it was suggested that in aluminosilicate melts there are discrete Si–O stretch bands near 1140 cm^{-1} for ≡Si(OAl) groups, near 1000 cm^{-1} for $=Si(OAl)_2$ groups, near 925 cm^{-1} for $-Si(OAl)_3$ groups and near 890 cm^{-1} for $Si(OAl)_4$ groups (see Fig. 6, McMillan et al., 1982). These groups are presumably spectroscopically analogous to the 1100-, 950-, 900- and 850-cm^{-1} stretch bands involving Si–O^- in melts on alkali and alkaline earth silicate melts (see p. 2031), although McMillan et al. (1982) emphasized (p. 2032) that their spectroscopic interpretation differs from a geometric interpretation. This interpretation does not result, therefore, in a distinction between Si–O^- vibrations (with which depolymerized units are identified) and Si–O° vibrations in Si–O–Al bridges (with which the position of aluminum in the aluminosilicate melts might be identified). The alternative spectroscopic interpretation is that the frequency of Si–O° stretch vibrations in three-dimensionally interconnected aluminosilicate melts decrease continuously as a function of Al/(Al+Si) of the melt. This decrease is either due to (Si,Al) coupling (Wright et al., 1966; Sharma et al., 1978b; Mysen et al., 1980a) or due to a decrease in the force constant of Si–O° stretching as a result of Si ⇌ Al substitution (Seifert et al., 1982a), or both. The relative merits of these spectroscopic models must be determined before the spectra in Figures 2–4 can be interpreted.

The model suggested by McMillan et al. (1982) (see also McMillan and Piriou, 1983) may be evaluated by comparing Raman spectra of binary metal oxide-silica glasses (as also done by Piriou and Alain, 1979) with those of three-dimensionally interconnected aluminosilicate glasses. It was initially suggested (Piriou and Alain, 1979; see McMillan et al., 1982, p. 2025) that the spectrum of $CaAl_2SiO_6$ (CATS) glass is similar to that of alkali metasilicate. Thus, one might interpret the spectrum of CATS glass on the basis of a metasilicate structure. This suggestion implies that because CATS can be considered a metasilicate only if one half of the Al^{3+} is a network former and the other half is a network modifier, from a spectroscopic point of view, 50% of the Al^{3+} must also be considered a network former and 50% a network modifier. If all Al^{3+} in the CATS stoichiometry behaved spectroscopically as alkali metals or alkaline earths, the spectrum would be similar to that of a pyrosilicate (3 nonbridging oxygens per silicon) rather than that of a metasilicate (2 nonbridging oxygens per silicon) as seems to be the suggested

Table 2. Hypothetical degree of polymerization (NBO/Si) of starting materials with Al^{3+} as a network modifier

	NS2	NS2(NA2)5	NS2(NA2)10	NS2(NA2)20	NS2(NA2)30
NBO/Si	1.0	1.26	1.53	2.01	2.73

basis for the spectroscopic interpretation of aluminosilicate glasses by McMillan et al. (1982). Thus, the suggested metasilicate basis for spectroscopic interpretation of CATS glass (see McMillan et al., 1982, p. 2025) is inconsistent with their *a priori* assumption (p. 2031) in which the oxygen in Si–O–Al is assumed to have the spectroscopic characteristics of a nonbridging oxygen. Instead, glasses of $NaAlSi_2O_6$ (Jd) and $Ca_{0.5}AlSi_2O_6$ (CA2S4) composition should be interpreted spectroscopically on the basis of a metasilicate structure. A comparison of spectra of CATS, CA2S4 and Jd glasses (at 1 atm) with those of metasilicate compositions is shown in Figure 5. The metasilicate compositions are $Ba_2Si_2O_6$ (BS), $Ca_2Si_2O_6$ (Wo), $CaMgSi_2O_6$ (Di) and $Mg_2Si_2O_6$ (En) (from Mysen et al., 1982a). Alkali metasilicate glasses are not included in this comparison because of the extreme difficulty in retaining alkali metals in the melts during preparation of sodium metasilicate glass (Kracek, 1930; Seifert et al., 1979a; Bigger, 1981) and the difficulties in documenting the glass composition after preparation. The spectra of alkali metasilicate glasses of Brawer and White (1975) do, however, closely resemble that of barium metasilicate (BS) composition in Figure 5. According to the spectroscopic model of McMillan et al. (1982), the spectra of Jd and CA2S4 (and perhaps CATS?) glass will resemble those of En, Di, Wo and BS composition at least in Raman band frequencies. Perhaps the most characteristic band of metasilicate glasses is the mixed bending and stretching band between 620 and 640 cm^{-1} (e.g., Etchepare, 1972; Brawer and White, 1975; Furukawa et al., 1981; McMillan and Piriou, 1983). The intensity of this band is 50% or more of that of the high-frequency envelope of the metasilicate glass spectra but is totally absent in the spectra of CATS, Jd and CA2S4 or any other three-dimensionally interconnected aluminosilicate glass spectrum (Fig. 5; see also Fig. 3 in Seifert et al., 1982a; and Figs. 3 and 7 in McMillan et al., 1982). Moreover, even without any deconvolution of the high-frequency envelopes of these spectra, it is evident that those of the metasilicate glasses show most of their intensity below 1000 cm^{-1} (primarily due to the stretch vibration from $Si–O^-$ bonds in SiO_3^{2-} units), whereas the aluminosilicate spectra that should be interpreted on the basis of metasilicate (whether CA2S4, Jd or, apparently, CATS) have most of their high-frequency envelope at 1000 cm^{-1} or higher. Thus, on the basis of the spectra of aluminosilicate and metasilicate glasses on which those of aluminosilicate glasses should be interpreted (e.g., McMillan et al., 1982, p. 2031) there is no resemblance. The inference is, therefore, that the Si–O bridging bonds in Si–O–Al bridges do not have spectroscopic characters resembling that of the Si–O bond in Si–O–M (where M is a network-modifying cation and the oxygen is nonbridging).

Results from molecular orbital calculations (e.g., de Jong and Brown, 1980) indicate that with an idealized T–O–T angle of 180°, the proportion of bonding electrons in the Si–O bridging bond of Si–O–Si and Si–O–Al is unaffected because of the charge-balance of Al^{3+} with metal cations. This conclusion is inconsistent with that of McMillan et al. (1982), who suggested that a formal charge of −1 could be assigned to the oxygen in Si–O–Al bridges in ≡Si(OAl), −2 in =Si(OAl)$_2$ and so on (p.

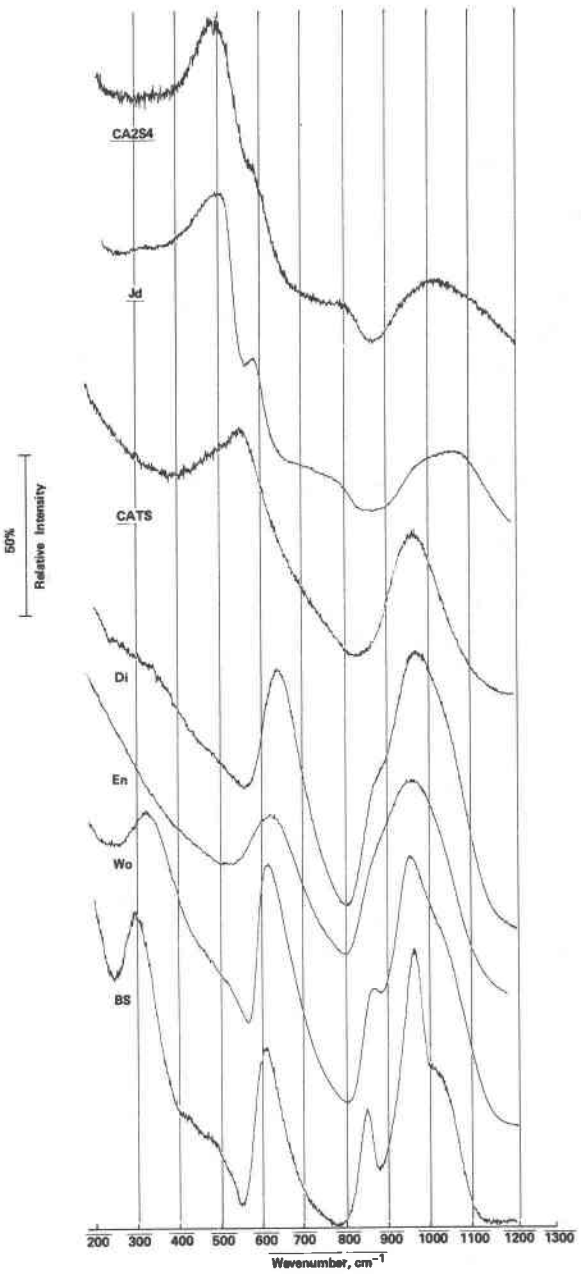

Fig. 5. Unpolarized spectra of metasilicate compositions $Ba_2Si_2O_6$ (BS), $Ca_2Si_2O_6$ (Wo), $CaMgSi_2O_6$ (Di), $Mg_2Si_2O_6$ (En) (from Mysen et al., 1982a) and the aluminosilicate compositions CATS ($CaAl_2SiO_6$), Jd ($NaAlSi_2O_6$) and CA2S4 ($Ca_{0.5}AlSi_2O_6$) (from Seifert et al., 1982a).

2035). The assignment of formal negative charge to the bridging oxygen in charge-balanced aluminosilicate systems does not have any foundation in the crystal chemistry of aluminosilicates either.

The T–O–T angle does, however, decrease with increasing charge-balanced Al^{3+} substitution (an average of 7° in crystalline aluminosilicates; Gibbs et al., 1981), resulting in a decrease in the proportion of bonding electrons in the Si–O bond (de Jong and Brown, 1980). The proportional decrease in bonding electrons results in a reduction in the Si–O bond strength and thus the force constant for stretching. This anticipated lowered bond strength is consistent with the approximately 20% decrease in force constants calculated by Seifert et al. (1982a) for Si–O stretching in quenched melts along the join SiO_2–$NaAlSiO_4$. This decrease in force constants results in a systematic and continuous decrease in stretch frequencies as a function of Si/Al of the tetrahedra in question. The conclusion does not, however, imply that the Si–O bond spectroscopically is like a nonbridging bond but simply that it will weaken as the neighboring tetrahedral silicon is replaced by aluminum. Whether (Si,Al) coupling of the vibrations from T–O bridging oxygen bonds may also affect the frequencies of the stretch vibrations cannot be determined. For the present discussion it is not important to decide which of the two mechanisms operates or whether both may be involved. Rather, it merely has to be established that the frequencies of relevant stretch vibrations depend on the Al/Si of the appropriate tetrahedron. Furthermore, the vibrations that result from nonbridging oxygens must be spectroscopically distinct from Si–O vibrations involving Si–O–Al bridges. In view of the above discussion and other published information (e.g., Brawer and White, 1975, 1977; Sharma et al., 1978b; Mysen et al., 1980a, 1982a; Furukawa et al., 1981; Seifert et al., 1982a), this distinction can be made.

The structural position of tetrahedral Al^{3+} in glasses on the join NS2–NA2

The Raman spectra of the quenched melts on the join $Na_2Si_2O_5$–$Na_4Al_2O_5$ (Figs. 2–4) show that increasing Al/(Al+Si) results in rapid disappearance of the 1150-cm^{-1} band (Si–O° stretch from three-dimensional SiO_2 units) and a decrease in the frequency of the 1070-cm^{-1} band coupled with an increase in its relative intensity (Table 1). This increase is associated with growth of a band near 560 cm^{-1}, which most likely is due to the presence of Al–O–Al bridges in these quenched melts (Seifert et al., 1982a; McMillan et al., 1982). The spectroscopic changes near 1000–1070 cm^{-1} probably result from increasing Al/(Al+Si) in the three-dimensional network units. This intensity increase may result partly from increasing relative abundance of aluminous, three-dimensional network units and partly from increasing Al/(Al+Si) of the three-dimensional network units. The frequencies of the 860-, 900- and 945-cm^{-1} bands are not affected by increasing Al/(Al+Si) of the melt. One may conclude, therefore, that the structural units with nbo/si = 4, 3 and 2 do not contain discernible amounts of Al^{3+}. Substitution of Al^{3+} for Si^{4+} in these units would result in a lowering of these Raman frequencies. The $Si_2O_5^{2-}$ unit, on the other hand, probably has some Al^{3+} at all pressures and temperatures for compositions NS2(NA2)20 and NS2(NA2)30 because the $Si–O^-$ stretch band near 1100 cm^{-1} shows a slight decrease in frequency relative to that of the $Si–O^-$ band from $Si_2O_5^{2-}$ units in melts with lower Al content. At 30 kbar, the frequency shift commences in spectra of quenched melts at NS2(NA2)10, a result indicating that at high pressures aluminum enters $Si_2O_5^{2-}$ units at lower Al/(Al+Si) of the melt.

The relative intensities of the $Si–O^-$ stretch bands from SiO_4^{4-} (860 cm^{-1}), $Si_2O_7^{6-}$ (900 cm^{-1}) and SiO_3^{2-} (945 cm^{-1}) units appear to increase relative to the total intensity of all the $Si–O^-$ stretch bands (Table 1). It seems, therefore, that the relative abundance of the most depolymerized units in the melts increases together with the increase in TO_2 (T = Al + Si) with increasing Al/(Al+Si) of the melt.

Solubility mechanism of aluminum in silicate melts

Aluminum occurs in tetrahedral coordination and primarily occupies structural units with a three-dimensionally interconnected network. This conclusion is in accord with that of Mysen et al. (1981a) for melts on the composition joins $Na_2Si_2O_5$–$NaAlO_2$, $Na_2Si_2O_5$–$CaAl_2O_4$ and $CaSi_2O_5$–$CaAl_2O_4$ at 1 atm and that of Dowty (1983) for aluminosilicate melts in general on theoretical grounds.

The preference of Al^{3+} for three-dimensional network units may be rationalized by comparing these inferences with the crystal chemical behavior of tetrahedrally coordinated Al^{3+} in aluminosilicate minerals. For example, Brown and Gibbs (1970) observed that in such minerals, Si^{4+} would occur in tetrahedral sites associated with T–O–T bridges with the widest possible range in T–O–T angle, whereas Al^{3+} shows a preference for sites associated with the smallest possible range in T–O–T angle and in fact the smallest value of this angle. Brown and Gibbs (1970) noted that this crystal-chemical behavior of Al^{3+} is seen in low albite, for example. In its crystal structure, Al^{3+} occurs principally in the $T_1(O)$ site, a site associated with a T–O–T angle 3–10° smaller than the other T–O–T angles (Brown et al., 1969; Stewart and Ribbe, 1969). In analogy with crystal chemistry, the T–O–T angle in the various types of silicate units decreases in the order $Si_2O_7^{6-} > SiO_3^{2-} > Si_2O_5^{2-} > SiO_2$. One may suggest that even though details in the geometry of coexisting $Si_2O_7^{6-}$, SiO_3^{2-}, $Si_2O_5^{2-}$ and SiO_2 units are not known in melts, a similar order exists (as also suggested by Furukawa et al., 1981). In that case, the preference of Al^{3+} for the most polymerized unit (SiO_2) may be understood.

Relative abundance of structural units

The relative abundance of individual structural units in the melts, X_i, can be obtained from the relative intensity data of Raman bands as given in Table 1. The relative intensity of each Raman band depends not only on the relative abundance of the structural unit containing the specific type of bonding that gives rise to the vibration, but also on the scattering properties of this bond (e.g., Long, 1977). Scattering properties cannot be determined routinely. Raman cross sections, which include geometry and polarizability of relevant bonds, may be determined empirically from a set of Raman spectral band intensities such as given in Table 1.

The procedure involves the solution of a system of linear equations with one unknown per structural unit in the melt. The relative intensities of the Raman bands, A_i, are related to the relative abundance (mole fraction), X_i, by;

$$X_i = A_i\alpha_i, \tag{2}$$

where α_i is the normalized Raman cross section. In the melts under discussion, there are N structural units, of which one has a three-dimensional network structure. Another equation:

$$\sum_{g=1}^{N-1} X_j = \sum_{j=1}^{N-1} A_j\alpha_j, \tag{3}$$

describes the mass balance of those N−1 structural units that contain nonbridging oxygen. The respective relative abundances (mole fractions) and relative intensities of Raman bands from Si–O^- bonds in structural units with nonbridging oxygens are X_j and A_j. For each sample, there is an additional conservation equation of the form:

$$\sum_{j=1}^{N-1} A_j\alpha_j\,(\text{nbo/t})_j = \text{NBO/T}, \tag{4}$$

where (nbo/t) is the number of nonbridging oxygen per tetrahedral cations in the individual structural unit and NBO/T is the bulk quantity. The compositional and structural use of the NBO/T is discussed further in the footnote in the introduction of this report.

The α_j factors are calculated for Si–O^- symmetric stretch vibrations. The three-dimensional network units are not included in equations 3 and 4 because its scattering efficiency is most likely a function of the Al content of this unit and because the scattering efficiency of bridging in Si–O bonds is so much smaller than those of the nonbridging bonds (Phillips, 1982) that the calculated value of α_{3D} is likely to be uncertain. The X_{3D} is determined instead from the difference:

$$X_{3D} = 1 - \sum_{j=1}^{N-1} X_j. \tag{5}$$

so that:

$$\sum_{i=1}^{N} X_i = X_{3D} + \sum_{j=1}^{N-1} X_j. \tag{6}$$

With these considerations in mind, the α_j factors are calculated from the relative intensities of the 900-, 945- and 1100-cm^{-1} bands normalized to their total intensity for melt compositions where there is little indication that Al^{3+} is in the $Si_2O_5^{2-}$ units (Table 1). Although it is difficult to assess the uncertainty in the calculated values of α_j, the results by Seifert et al. (1981b) and Mysen et al. (1982b) indicate that bulk melt NBO/T-values of binary $CaO–SiO_2$ melts calculated with this method are within 5% (relative) of those calculated from the Ca/Si. The statistical quality of the present spectra is comparable to that of Seifert et al. (1981b) and Mysen et al. (1982b). Thus, a 5% relative uncertainty in the α_j-values obtained here most probably is a maximum.

The scattering efficiency of Si–O^- bonds from $Si_2O_5^{2-}$ units with some (unknown amount of) Al^{3+} substituted for Si^{4+} is not known. Its value probably would be smaller than in the absence of Si^{4+}, but for the present calculations this scattering efficiency is considered constant. Finally, there is a small proportion of SiO_4^{4-} units in the most aluminous melts. The proportion of this unit appears to increase with increasing pressure (Table 1; Figs. 2–4). The value of $\alpha_{SiO_4^{4-}}$ cannot be calculated accurately because the 860-cm^{-1} band (Si–O^- stretching in SiO_4^{4-} units) can be resolved only in spectra where the frequency of the 1100-cm^{-1} band (Si–O^- stretching in $Si_2O_5^{2-}$ units) is slightly Al/(Al+Si) dependent. Its value is, however, unlikely to be greater than that of the $Si_2O_7^{6-}$ unit (0.33). It is assumed to be 0.3 for the present calculation. Although this assumption results in an uncertainty in the absolute value of the abundance of SiO_4^{4-} units, the small value of the α_j factor itself and the low relative intensity of the 860-cm^{-1} band result in only a small uncertainty in the relative abundance of the other units in the melts.

Results of such calculations (Fig. 6) indicate that under all conditions studied, with increasing bulk melt Al/(Al+Si) the relative abundance of units with NBO/T = 1 decreases significantly. The relative abundance of three-dimensional network units increases. Mass-balance calculations of Al/(Al+Si) and the data in Figure 6 indicate that even with bulk melt Al/(Al+Si) = 0.1, the Al/(Al+Si) of the TO_2 unit exceeds 0.6. The changes in relative abundance of coexisting structural units agree, in principle, with the suggestion of Dowty (1983) and data of Mysen et al. (1981a). The latter data are not directly comparable with the present results, however, because in the experiments of Mysen et al. (1981a), aluminum was added in the form of $NaAlO_2$ and $CaAl_2O_4$. As a result, increasing Al/(Al+Si) was coupled with a decrease in bulk melt NBO/T. Those data did indicate, however, that

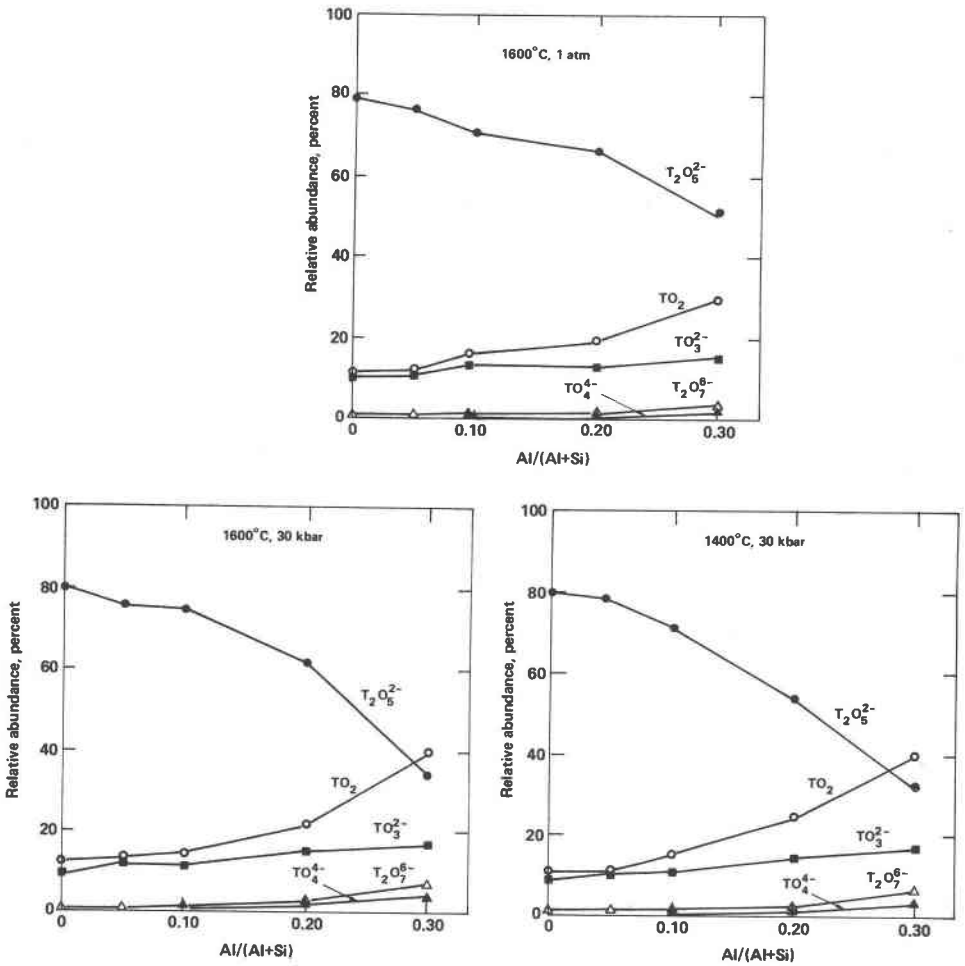

Fig. 6. Relative abundance of anionic units in melts on the composition join NS2-NA2 as a function of NA2 content, temperature and pressure. Symbols on curves: TO_2, three-dimensional network units; $T_2O_5^{2-}$, structural units with average nbo/t = 1; TO_3^{2-}, structural units with average nbo/t = 2; $T_2O_7^{6-}$, relative abundance of structural units with nbo/t = 3; TO_4^{4-}, relative abundance of units with nbo/t = 4. As indicated in the text, in three-dimensional network units, T = Al + Si. At 30 kbar and 1600°C, T = Si + Al in melts with Al/(Al + Si) > 0.1. Most probably, in all other units T = Si.

Al^{3+} shows a distinct preference for the most polymerized units in the melt although this preference becomes less pronounced with increasing Ca/Na.

The increase in the relative abundance of three-dimensional network units and the decrease in abundance of units with nbo/si = 1 are compensated for by an increase in the relative abundance of units with nbo/si > 1 (Fig. 6). This compensation is necessary in order to maintain the same NBO/T of the melt. In its simplest form, the relative change in abundance may be expressed with the equation

$$Si_2O_5^{2-}(1) + (NaAl)_2O_5^{2-}(1) = 2SiO_3^{2-}(2) + 2NaAlO_2(0), \quad (7)$$

where (0), (1) and (2) represent the nbo/t values of the anionic units expressed with that stoichiometry. Analogous expressions may be written for structural changes involving units with nbo/t > 2 and also to account for variable Al/(Al+Si) of the structural units (principally the three-dimensional network units).

For melts quenched from 1600°C and 1 atm the compensation for increased abundance of the three-dimensional network units is accomplished predominantly with increasing relative abundance of SiO_3^{2-} units, with only a small increase in the proportion of more depolymerized structural units. At 30 kbar the adjustment of the relative abundance of the structural units with increasing bulk melt Al/(Al+Si) is more pronounced. For example, at 30 kbar and 1400°C, only 30% of the melt structure is comprised of $Si_2O_5^{2-}$ units in quenched NS2(NA2)30 melt as compared with 40% at 30 kbar and 1600°C and about 60% at 1600°C and 1 atm. The relative abundance of the highly depolymerized units (SiO_4^{4-} and

$Si_2O_7^{6-}$) is also greater in melts quenched at 30 kbar. This difference in relative stability as a function of pressure and temperature stems from (1) diminished stability of $Si_2O_5^{2-}$ units with increasing pressure or decreasing temperature, or (2) an increase in Al/(Al+Si) of the three-dimensional network units with increasing pressure or decreasing temperature, or (3) both. In any case, the additional shift to the right of an expression similar to equation 5 with increasing pressure and decreasing temperature is anticipated.

Aluminum distribution between immiscible titanium- and iron-bearing melts

The strong preference of Al^{3+} for the most polymerized structural unit in the melts reported here (Fig. 6) and elsewhere (Mysen et al., 1981a) is in apparent conflict with the suggestion of Hess and Wood (1982). They determined the distribution of Al^{3+} between coexisting immiscible melts in the system CaO–MgO–FeO–TiO_2–Al_2O_3–SiO_2 and found that Al^{3+} was preferred by the least polymerized of the two melts. Hess and Wood (1982) did not consider the Al^{3+}-distribution data of Visser and Koster van Groos (1979) for the system K_2O–FeO–Al_2O_3–TiO_2–SiO_2 (p. 972). In that system Al^{3+} showed a preference for the most polymerized of two coexisting immiscible melts (the weight ratio of Al_2O_3 between the coexisting melts ranged from 1.1 to 5.3).

The present data set results in similar apparent discrepancies with the results of Hess and Wood (1982). It appears, therefore, that rather than resulting from misinterpretation of data, the different behavior of Al^{3+} in the various systems may be due to the very large differences in chemical compositions of the liquids in the two studies on Al^{3+} partitioning and the two Raman studies. There are several important differences in bulk chemistry in these systems. The charge-balancing cations for Al^{3+} in the data set of Hess and Wood (1982) were Ca^{2+}, Mg^{2+} and possibly Fe^{2+}, a difference that may affect the extent of Al^{3+} preference. It has been shown (Navrotsky et al., 1982) that the relative stability of three-dimensional aluminosilicate complexes decreases in the order K > Na > Ca > Mg. The preference of Al^{3+} for three-dimensional network units in the system Na_2O–CaO–Al_2O_3–SiO_2 becomes less pronounced with increasing Ca/Na (Mysen et al., 1981a), in agreement with the conclusion of Navrotsky et al. (1982). The charge-balancing cation of Al^{3+} in the study of Visser and Koster van Groos (1979) was K^+, probably resulting in more stable aluminosilicate complexes than in the chemical compositions studied by Hess and Wood (1982). This difference in the charge-balancing cation may at least partly account for the qualitative differences between the present results, those of Mysen et al. (1981a) and Visser and Koster van Groos (1979) on the one hand, and those of Hess and Wood (1982) on the other.

The silicate melts in the experiments of Hess and Wood (1982) contained large amounts of TiO_2 (9.65–24.68 wt.% TiO_2 in the least polymerized melt and 2.98–7.39 wt % in the most polymerized melt). In the experiments of Visser and Koster van Groos (1979) the TiO_2 in coexisting immiscible melts in the system K_2O–FeO–Al_2O_3–SiO_2 (and inverse partitioning behavior of Al^{3+}) was typically about 50% of that in the experiments of Hess and Wood (1982). Thus, it appears that Al^{3+} distribution in more complex melts depends on the Ti^{4+} content as well as the available metal cations for Al^{3+} charge-balance. As already mentioned, neither the present data nor those of Mysen et al. (1981) were obtained with Ti^{4+} in the system. The relationship between Ti^{4+} content and Al^{3+} distribution may be at least partly explained by the observation (Mysen et al., 1980b) that Ti^{4+} in aluminosilicate melts forms aluminotitanate complexes (even in the system $NaAlSi_3O_8$–TiO_2). Dickenson and Hess (1983) suggested, on the basis of redox ratio determinations of iron in the system K_2O–Al_2O_3–SiO_2–Fe–O–TiO_2, that Ti^{4+} may form complexes with K^+ rather than with Al^{3+}. These redox data can, however, be explained equally well by aluminum titanate complexing because $Fe^{3+}/\Sigma Fe$ of silicate melts is also positively correlated with Al/(Al+Si) of the silicate network (Neumann et al., 1982; Seifert et al., 1982b; Mysen and Virgo, 1983; Mysen et al., 1984). Formation of aluminotitanate complexes will be accompanied by a decrease in the Al/(Al+Si) of the aluminosilicate network. Thus, the observations by Dickenson and Hess (1983) are consistent with aluminum titanate complexing in the melts. The relative stabilities of aluminosilicate and aluminotitanate complexes with different cations for Al^{3+} charge-balance is not known but is likely to depend strongly on the type of charge-balancing cations present (Mysen et al., 1981a; see also Navrotsky et al., 1982). Consequently, suggestions as to the relationships between element distribution of this kind and the chemical complexities introduced by Hess and Wood (1982) are premature at this stage and should await evaluations of the structural roles of all components involved.

Properties of aluminosilicate melts

Aluminum is in tetrahedral coordination in aluminosilicate melts with $M^+ \geq Al^{3+}$ or $M^{2+} \geq 2Al^{3+}$ (see also Seifert et al., 1982a; McMillan et al., 1982; Navrotsky et al., 1982; Mysen et al., 1982a). The $Al^{3+} \rightleftharpoons Si^{4+}$ substitution in melts where this compositional requirement is met does not, therefore, affect the NBO/T of the melt. Substitution of Al^{3+} for Si^{4+} results in decreasing activity of silicate components in the melts simply because of the dilution of Si^{4+}-components with possible Al^{3+}-analogs. One might expect, therefore, that the liquidus fields of aluminosilicate minerals (e.g., feldspars) and those of Al-free, depolymerized minerals (e.g., meta- and orthosilicates) expand as the Al/(Al+Si) increases. This principal effect is illustrated in Figure 7, where the liquidus boundaries of minerals with different polymerization shift to less polymerized compositions (negative change of NBO/T) with increasing Al/(Al+Si). In this figure, the

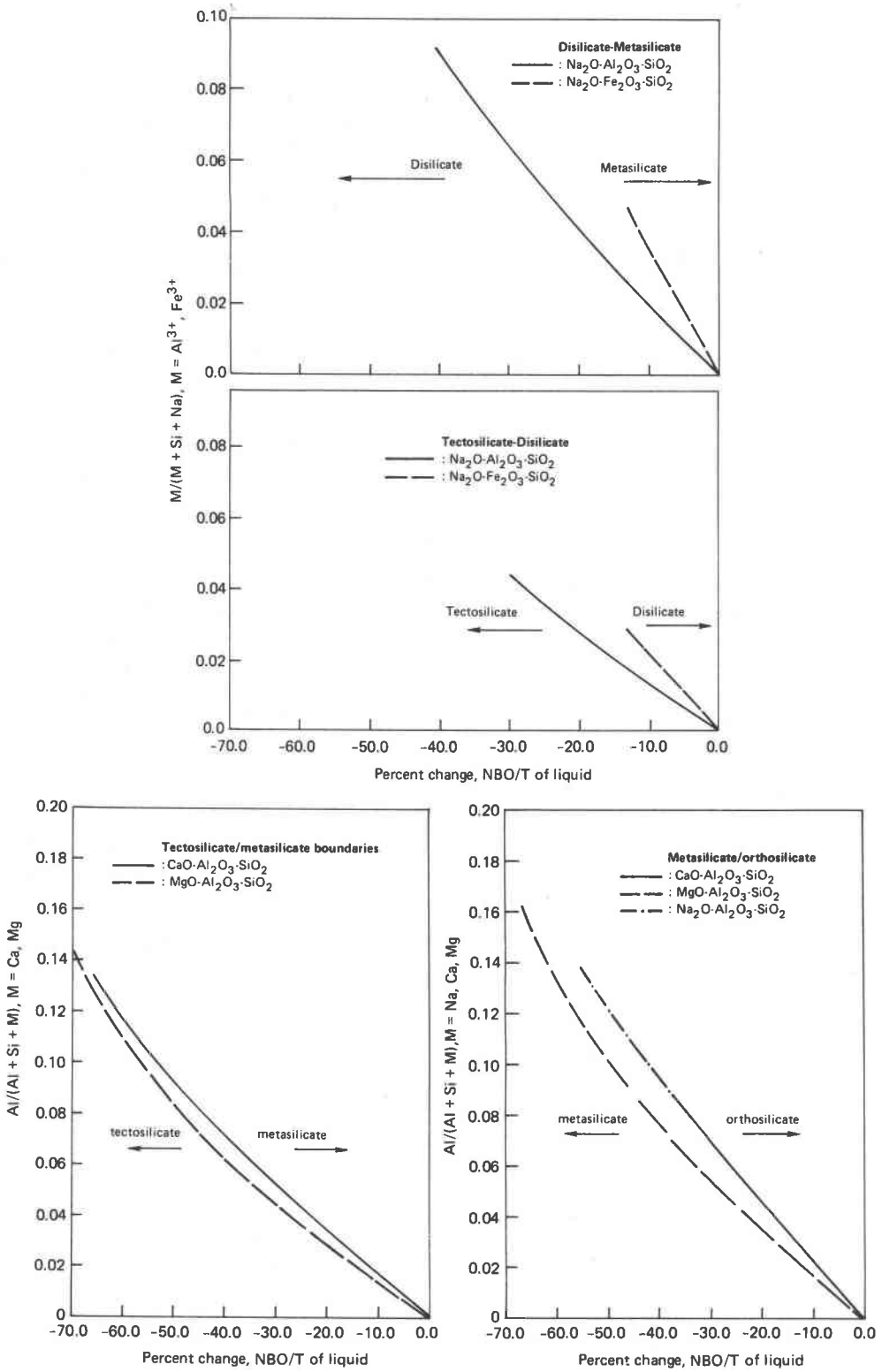

Fig. 7. Relative change (percent relative to value in Al-free systems) of non-bridging oxygens per tetrahedrally-coordinated cations (NBO/T) of liquids along the tectosilicate-disilicate, tectosilicate-metasilicate and metasilicate-orthosilicate liquidus boundaries in the systems Na_2O–Al_2O_3–SiO_2, Na_2O–Fe_2O_3–SiO_2, CaO–Al_2O_3–SiO_2 and MgO–Al_2O_3–SiO_2 (derived from phase equilibrium data of Osborn and Muan, 1960a,b,c and Bowen et al., 1930). Both ferric iron and aluminum are considered in tetrahedral coordination in all melts (for structural data relevant to the melt systems, see also Brown et al., 1978; Seifert et al., 1979b; Mysen and Virgo, 1983; Taylor and Brown, 1979a,b; Seifert et al., 1982a).

lines are terminated at the intersection of the relevant liquidus boundaries with the liquidus boundary involving an aluminosilicate mineral. It is noted, however, that the magnitude of the shifts depends on the type of metal cation (Mg, Ca or Na), thus perhaps suggesting that the proportions of the anionic units and the distribution of Al^{3+} between the units in the melts affect the position of the liquidus boundaries. The relative stabilities of these minerals depend on both the thermodynamic properties of the minerals and the melt only partly. The properties of the melts will reflect the distribution of Al^{3+} between the individual structural units. For a melt composition of given NBO/T and Al/(Al+Si), the proportions of the individual units depend, for example on the extent of Al^{3+} preference for three-dimensional network units. For disilicate compositions, for example (NBO/T = 1), the proportions of aluminous, three-dimensional network units and the proportions of Al-free structural units with nbo/si > 1 increase with increasing Al/(Al+Si) of the system (see also Fig. 6).

Extension of the present structural data to magmatic liquids requires consideration of Ca^{2+} and Mg^{2+} for charge-balance of Al^{3+}. As also indicated above, the relative stabilities of Ca^{2+}- and Mg^{2+}-charge-balanced aluminosilicate complexes are less than those of Na^+-stabilized aluminosilicates (Navrotsky et al., 1982). This difference is probably reflected in the less pronounced distribution of Ca^{2+}-charge-balanced Al^{3+} between coexisting structural units compared with that of Na^+-charge-balanced Al^{3+} in silicate melts (Mysen et al., 1981a). In addition, the type of network-modifying cation affects the relative abundance of anionic units in the melt. For example, in binary metal oxide-silica melts of disilicate stoichiometry, the $Si_2O_5^{2-}/(SiO_3^{2-} + SiO_4^{4-} + SiO_2)$ decreases rapidly with increasing Z/r^2 of the metal cation Mysen et al., 1982a). In an $MgSi_2O_5$ melt, for example, it is unlikely that $Si_2O_5^{2-}$ units are stable. Kirkpatrick (1983) and Kirkpatrick et al. (1981) pointed out that typical basaltic melts have NBO/T between 0.7 and 0.9. In most binary metal oxide-silica melts, compositions with this NBO/T have little or no abundance of SiO_4^{4-} units. In fact, on both the joins $MgO–SiO_2$ and $CaO–SiO_2$ (Greig, 1927; Phillips and Muan, 1959) compositions in the range of NBO/T comparable to basaltic liquid show liquid immiscibility. Basaltic liquids apparently, however, do have SiO_4^{4-} units in the melt (see also Burnham, 1981), and liquid immiscibility is not particularly common. These suggested differences in liquid structure of basaltic liquids as indicated by their liquidus phase equilibria and those of melts on binary metal oxide-silica joins may be explained by the Al content of the basalt compositions [Al/(Al+Si) typically is about 0.25; Chayes, 1975]. It can be seen from the phase equilibria in the systems $CaO–Al_2O_3–SiO_2$ and $MgO–Al_2O_3–SiO_2$ (Osborn and Muan, 1960b,c) that this level of Al/(Al+Si) results in complete disappearance of the liquid immiscibility field.

The aluminum content of basaltic magmatic liquids may also help explain the apparent expansion of the olivine liquidus field compared with the orthosilicate liquidus fields of binary silicate systems and the apparent absence of SiO_4^{4-} units in the relevant melt compositions. Regardless of whether Na^+, Ca^{2+} or Mg^{2+} charge-balances Al^{3+} in tetrahedral coordination, this Al^{3+} probably will show a strong preference for three-dimensional network units in the melt. For Ca^{2+} or Mg^{2+} charge-balanced Al^{3+}, this unit probably approximates $Al_2Si_2O_8^{2-}$ stoichiometry (Seifert et al., 1982a; see also McMillan et al., 1982, and Navrotsky et al., 1982, for discussion of ordering in alkaline earth aluminate-silica melts). The excess silica over Si/Al = 1 probably occurs as SiO_2 units. In alkaline earth systems the nonbridging oxygens in the melts exist predominantly as SiO_4^{4-}, $Si_2O_7^{6-}$ and SiO_3^{2-} units. Thus, increasing Al/(Al+Si) of aluminosilicate melts results in an increase in the abundance of these units. For Na^+ charge-balanced Al^{3+}, the preference of aluminum for the three-dimensional network units is stronger than in the Ca^{2+} system (Mysen et al., 1981a). Thus, the concentration of three-dimensional aluminosilicate units in alkali aluminosilicate melts increases more rapidly with increasing Al/(Al+Si) than in alkaline earth aluminosilicate melts. In this case, the abundance of the depolymerized units also increases. It is suggested, therefore, that the large olivine liquidus field in basaltic magma at least partly is related to the partitioning of Al^{3+} in three-dimensional network units with a concomitant increase in the relative abundance of depolymerized units such as orthosilicate.

It has also been observed, however, that some basaltic liquids have plagioclase on their liquidus, whereas others do not (Fig. 8). In the two compositions in Figure 8 (Kushiro and Thompson, 1972) both liquid compositions have similar bulk melt NBO/T and Al/(Al+Si). The melt with plagioclase on the liquidus has, however, $M^+/(M^+ + M^{2+})$ about 60% higher. It is suggested that this difference in liquidus mineralogy results at least partly from the stronger partitioning of Al^{3+} into the three-dimensional network units in the alkali-rich basalt. This preference causes a higher activity of aluminosilicate component in the melt, thus resulting in plagioclase, rather than olivine on the liquidus.

An increase in the compressibility and thermal expansion of silicate melts on binary metal oxide–silica joins has been related to increases in the abundance of three-dimensional network units in silicate melts (Bockris and Kojonen, 1960; MacKenzie, 1960; Scarfe et al., 1979). The present data indicate that silicate melts with the same NBO/T are likely to become more compressible as their Al content is increased.

The pressure dependence of melt viscosity becomes more pronounced with decreasing NBO/Si (Scarfe et al., 1979) at least on binary metal oxide–silica joins. One may speculate, therefore, that as Al^{3+} is exchanged for Si^{4+} in

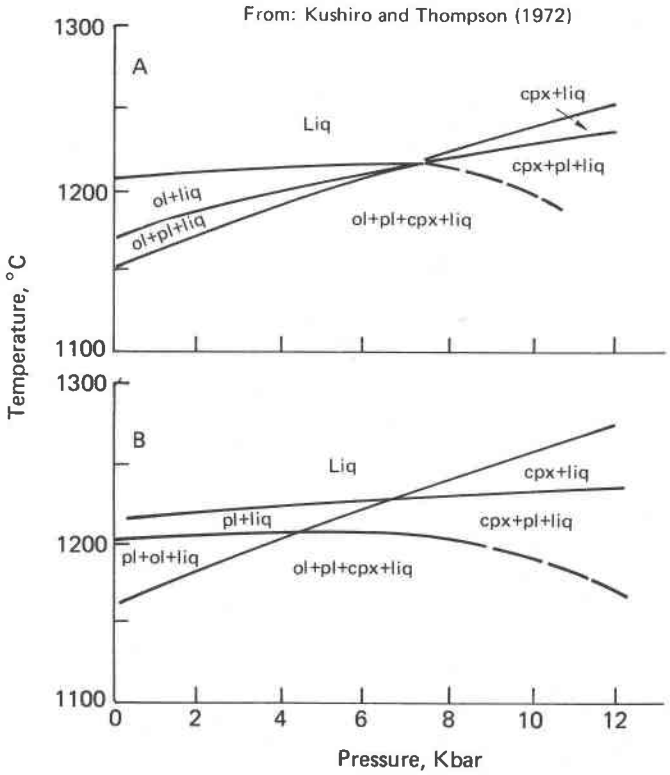

Compositional Features

	A	B
SiO_2	49.68	49.89
TiO_2	1.55	1.35
Al_2O_3	15.49	16.70
Fe_2O_3	0.92	1.55
FeO	8.25	7.75
MnO	0.18	0.19
MgO	9.17	7.44
CaO	10.61	10.90
Na_2O	2.88	3.01
K_2O	0.11	0.23
$M^+/M^+ + M^{2+}$	0.151	0.257
Al/(Al+Si)	0.269	0.283
NBO/T	0.739	0.690

Fig. 8. Portions of temperature–pressure equilibria of two basaltic liquids with different values of $M^+/(M^+ + M^{2+})$ (after Kushiro and Thompson, 1972).

a silicate melt (without altering bulk melt NBO/T) the pressure dependence of the melt viscosity increases. This increase is due not only to the increasing bulk melt Al/(Al+Si) but also to the increased relative abundance of three-dimensional network units as the bulk melt Al/(Al+Si) or pressure is increased. In analogy with the viscosity data of three-dimensional melts on the joins $NaAlO_2$–SiO_2 and $CaAl_2O_4$–SiO_2 (Kushiro, 1978, 1980, 1981), the effect of substituted Al^{3+} is much greater for Na^+-balanced than Ca^{2+}-balanced melts. As a result, one would expect that the pressure dependence of the viscosity of aluminosilicate melts is more pronounced the higher their alkali content.

Acknowledgments

Critical reviews by R. M. Hazen, P. McMillan and H. S. Yoder, Jr. are appreciated.

References

Bigger, G. M. (1981) Na_2O mobility in one-atmosphere quench furnaces. Progress in Experimental Petrology, Fifth Progress Report of Research Supported by NERC (1978–1980), 89–90.

Bockris, J. O. and Kojonen, F. (1960) Compressibility of certain molten alkali silicates and borates. Journal of the American Ceramic Society, 82, 4493–4497.

Bockris, J. O., MacKenzie, J. D. and Kitchner, J. A. (1955) Viscous flow in silica and binary liquid silicates. Transactions of the Faraday Society, 51, 1734–1748.

Bottinga, Y., Weill, D. F. and Richet, P. (1981) Thermodynamic modeling of silicate melts. In R. C. Newton, A. Navrotsky and B. J. Wood, Eds., Thermodynamics of Minerals and Melts, p. 207–245. Springer Verlag, New York, Heidelberg, Berlin.

Bowen, N. L., Schairer, J. F. and Willems, H. W. V. (1930) The ternary system Na_2SiO_3–Fe_2O_3–SiO_2. American Journal of Science, 20, 405–455.

Boyd, F. R. and England, J. L. (1960) Apparatus for phase equilibrium measurements at pressures up to 50 kilobars and temperatures up to 1750°C. Journal of Geophysical Research, 65, 741–748.

Brawer, S. A. and White, W. B. (1975) Raman spectroscopic investigation of the structure of silicate glasses. I. The binary silicate glasses. Journal of Chemical Physics, 63, 2421–2432.

Brawer, S. A. and White, W. B. (1977) Raman spectroscopic investigation of the structure of silicate glasses. II. Soda-alkaline earth-alumina ternary and quaternary glasses. Journal of Non-Crystalline Solids, 23, 261–278.

Brown, G. E. and Gibbs, G. V. (1970) Stereochemistry and ordering in the tetrahedral position of silicates. American Mineralogist, 55, 1587–1607.

Brown, G. E., Gibbs, G. V. and Ribbe, P. H. (1969) The nature and variation in length of the Si–O and Al–O bonds in framework silicates. American Mineralogist, 54, 1044–1061.

Brown, G. E., Keefer, K. D. and Fenn, P. M. (1978) Extended X-ray fine structure (EXAFS) study of iron-bearing silicate

glass (abstr.) Annual Meeting, Geological Society of America, 373.

Burnham, C. W. (1974) $NaAlSi_3O_8$–H_2O solutions. A thermodynamic model for hydrous magmas. Bulletin de Minéralogie, 97, 223–230.

Burnham, C. W. (1981) The nature of multicomponent aluminosilicate melts. Physics and Chemistry of the Earth, 13–14, 197–227.

Chayes, F. (1975) Average composition of commoner Cenozoic volcanic rocks. Carnegie Institution of Washington Year Book, 74, 547–549.

de Jong, B. H. W. S. and Brown, G. E. (1980) Polymerization of silicate and aluminate tetrahedra in glasses and aqueous solutions.—II. The network-modifying effects of Mg^{2+}, K^+, Na^+, Li^+, H^+, OH^-, F^-, Cl^-, H_2O, CO_2 and H_3O^+ on silicate polymers. Geochimica et Cosmochimica Acta, 44, 1627–1643.

Dickenson, M. P. and Hess, P. C. (1983) Fe redox equilibria and the structural role of P^{5+}, Ti^{4+} and Fe^{3+}. (abstr.) EOS, 64, 350.

Domine, F. and Piriou, B. (1983) Study of sodium silicate melt and glass by infrared spectroscopy. Journal of Non-Crystalline Solids, 55, 125–131.

Dowty, E. (1983) Aluminum tetrahedra in silicate glasses: Normal-coordinate vibrational analysis. (abstr.) EOS, 64, 344.

Etchepare, J. (1972) Study by Raman spectroscopy of crystalline and glassy diopside. In R. W. Douglas and B. Ellis, Eds., Amorphous Materials, p. 337–346. Wiley, New York.

Fox, K. E., Furukawa, T. and White, W. B. (1982) Transition metal ions in silicate melts. Part 2. Iron in sodium silicate glasses. Physics and Chemistry of Glasses, 23, 169–178.

Furukawa, T., Fox, K. E. and White, W. B. (1981) Raman spectroscopic investigation of the structure of silicate glasses. III. Raman intensities and structural units in sodium silicate glasses. Journal of Chemical Physics, 75, 3226–3237.

Gaskell, D. M. (1982) The densities and structures of silicate melts. In S. K. Saxena, Ed., Advances in Physical Geochemistry, Vol. 2, p. 153–157. Springer Verlag, New York.

Gibbs, G. V., Meagher, E. P., Newton, M. D. and Swanson, D. K. (1981) A comparison of experimental and theoretical bond-length and angle-variations for minerals, inorganic solids and molecules. In M. O'Keeffe and A. Navrotsky, Eds., Structure and Bonding in Crystals, p. 195–225. Academic Press, New York.

Greig, J. W. (1927) Immiscibility in silicate melts. American Journal of Science, 13, 133–155.

Hess, P. C. and Wood, M. I. (1982) Aluminum coordination in metaaluminous and peralkaline silicate melts. Contributions to Mineralogy and Petrology, 81, 103–112.

Kirkpatrick, R. J. (1983) Theory of nucleation in silicate melts. American Mineralogist, 68, 66–78.

Kirkpatrick, R. J., Kuo, L.-C. and Melchior, J. (1981) Crystal growth in incongruently-melting compositions: Programmed cooling experiments with diopside. American Mineralogist, 66, 223–242.

Kracek, F. C. (1930) The system sodium oxide-silica. Journal of Physical Chemistry, 34, 1583–1598.

Kushiro, I. (1975) On the nature of silicate melt and its significance in magma genesis: Regularities in the shift of liquidus boundaries involving olivine, pyroxene, and silica minerals. American Journal of Science, 275, 411–431.

Kushiro, I. (1978) Viscosity and structural changes of albite ($NaAlSi_3O_8$) melt at high pressures. Earth and Planetary Science Letters, 41, 87–91.

Kushiro, I. (1980) Viscosity, density, and structure of silicate melts at high pressures, and their petrological applications. In R. B. Hargraves, Ed., Physics of Magmatic Processes, p. 93–121. Princeton University Press, Princeton.

Kushiro, I. (1981) Viscosity change with pressure of melts in the system CaO–Al_2O_3–SiO_2. Carnegie Institution of Washington Year Book, 80, 339–341.

Kushiro, I. and Thompson, R. N. (1972) Origin of some abyssal tholeiites from Mid-Atlantic Ridge. Carnegie Institution of Washington Year Book, 71, 403–406.

Lazarev, A. N. (1972) Vibrational Spectra and Structure of Silicates. Consultants Bureau, New York.

Long, D. A. (1977) Raman Spectroscopy. McGraw-Hill Book Company, New York.

MacKenzie, J. D. (1960) Structure of some inorganic glasses from high temperatures. In J. D. MacKenzie, Ed., Modern Aspects of the Vitreous State, p. 188–218. Butterworths, Washington, D.C.

McMillan, P. and Piriou, B. (1983) Raman spectroscopic studies of silicate and related glass structure: A review. Bulletin de Minéralogie, 106, 57–77.

McMillan, P., Piriou, B. and Navrotsky, A. (1982) A Raman spectroscopic study of glasses along the joins silica-calcium aluminate, silica-sodium aluminate and silica-potassium aluminate. Geochimica et Cosmochimica Acta, 46, 2021–2037.

Mysen, B. O. and Virgo, D. (1983) Redox equilibria, structure and melt properties in the system Na_2O–Al_2O_3–SiO_2–Fe–O. Carnegie Institution of Washington Year Book, 82, 313–317.

Mysen, B. O., Virgo, D. and Scarfe, C. M. (1980a) Relations between anionic structure and viscosity of silicate melts—a Raman spectroscopic study. American Mineralogist, 65, 690–710.

Mysen, B. O., Ryerson, F. J. and Virgo, D. (1980b) The influence of TiO_2 on the structure and derivative properties of silicate melts. American Mineralogist, 65, 1150–1165.

Mysen, B. O., Virgo, D. and Kushiro, I. (1981a) The structural role of aluminum in silicate melts—a Raman spectroscopic study at 1 atmosphere. American Mineralogist, 66, 678–701.

Mysen, B. O., Ryerson, F. J. and Virgo, D. (1981b) The structural role of phosphorous in silicate melts. The American Mineralogist, 66, 106–117.

Mysen, B. O., Virgo, D. and Seifert, F. A. (1982a) The structure of silicate melts: Implications for chemical and physical properties of natural magma. Reviews of Geophysics and Space Physics, 20, 353–383.

Mysen, B. O., Finger, L. W., Seifert, F. A. and Virgo, D. (1982b) Curve-fitting of Raman spectra of amorphous materials. American Mineralogist, 67, 686–696.

Mysen, B. O., Virgo, D. and Seifert, F. A. (1984) Redox equilibria of iron in alkaline earth silicate melts: Relationship between melt structure, oxygen fugacity, temperature and properties of iron-bearing silicate liquids. American Mineralogist, 69, 834–847.

Navrotsky, A., Hon, R., Weill, D. F. and Henry, D. J. (1980) Thermochemistry of glasses and liquids in the systems $CaMgSi_2O_6$–$CaAl_2Si_2O_8$–$NaAlSi_3O_8$, SiO_2–$CaAl_2Si_2O_8$–$NaAlSi_3O_8$ and SiO_2–Al_2O_3–CaO–Na_2O. Geochimica et Cosmochimica Acta, 44, 1409–1425.

Navrotsky, A., Peraudeau, P., McMillan, P. and Coutoures, J.-P. (1982) A thermochemical study of glasses and crystals along the joins silica-calcium aluminate and silica-sodium aluminate. Geochimica et Cosmochimica Acta, 46, 2039–2049.

Neumann, E.-R., Mysen, B. O., Virgo, D. and Seifert, F. A.

(1982) Redox equilibria of iron in melts in the system CaO–Al_2O_3–SiO_2–Fe–O. Carnegie Institution of Washington Year Book, 81, 353–355.

Osborn, E. F. and Muan, A. (1960a) Phase Equilibrium Diagrams of Oxide Systems. Plate 4. The System Na_2O–Al_2O_3–SiO_2. American Ceramic Society, Columbus, Ohio.

Osborn, E. F. and Muan, A. (1960b) Phase Equilibrium Diagrams of Oxide Systems. Plate 2. The System CaO–Al_2O_3–SiO_2. American Ceramic Society, Columbus, Ohio.

Osborn, E. F. and Muan, A. (1960c) Phase Equilibrium Diagrams of Oxide Systems. Plate 3. The System MgO–Al_2O_3–SiO_2. American Ceramic Society, Columbus, Ohio.

Phillips, B. and Muan, A. (1959) Phase equilibria in the system CaO–iron oxide–SiO_2 in air. Journal of the American Ceramic Society, 42, 413–423.

Phillips, J. C. (1982) Spectroscopic and morphological structure of tetrahedral glasses. Solid State Physics, 37, 93–171.

Piriou, B. and Alain, P. (1979) Density of states and structural forms related to physical properties of amorphous solids. High Temperatures–High Pressures, 11, 407–414.

Riebling, E. F. (1966) The structure of sodium aluminosilicate melts containing at least 50 mole % SiO_2 at 1500°C. Journal of Chemical Physics, 44, 2857–2865.

Rontgen, H., Wintergaher, P. and Kammel, R. (1960) Struktur und Eigenschaften von Schlacken der Metallhuttenprozesse. II. Viskositatsmessungen an Schmelzen der System Eisenoxydul-Kalk-Kieselsaure und Eisenoxydul-Kalk-Tonerde-Kieselsaure. Zeitschrift für Erzbergbau und Metallhuettenwesen, 8, 363–373.

Ryerson, F. J. and Hess, P. C. (1980) The role of P_2O_5 in silicate melts. Geochimica et Cosmochimica Acta, 44, 611–625.

Scarfe, C. M., Mysen, B. O. and Virgo, D. (1979) Changes in viscosity and density of melts of sodium disilicate, sodium metasilicate and diopside composition with pressure. Carnegie Institution of Washington Year Book, 78, 547–551.

Seifert, F., Virgo, D. and Mysen, B. O. (1979a) Sodium loss from sodium metasilicate melts in CO_2 and CO atmospheres. Carnegie Institution of Washington Year Book, 78, 679.

Seifert, F. A., Virgo, D. and Mysen, B. O. (1979b) Melt structures and redox equilibria in the system Na_2O–FeO–Fe_2O_3–Al_2O_3–SiO_2. Carnegie Institution of Washington Year Book, 78, 511–519.

Seifert, F. A., Mysen, B. O. and Virgo, D. (1981a) Structural similarity of glasses and melts relevant to petrological processes. Geochimica et Cosmochimica Acta, 45, 1879–1884.

Seifert, F. A., Mysen, B. O. and Virgo, D. (1981b) Quantitative determination of proportions of anionic units in silicate melts. Carnegie Institution of Washington Year Book, 80, 301–302.

Seifert, F. A., Mysen, B. O. and Virgo, D. (1982a) Three-dimensional network melt structure in the systems SiO_2–$NaAlO_2$, SiO_2–$CaAl_2O_4$ and SiO_2–$MgAl_2O_4$. American Mineralogist, 67, 696–718.

Seifert, F. A., Mysen, B. O., Virgo, D. and Neumann, E.-R. (1982b) Ferric–ferrous equilibria in melts in the system MgO–Al_2O_3–SiO_2–Fe–O. Carnegie Institution of Washington Year Book, 81, 355–357.

Sharma, S. K., Virgo, D. and Mysen, B. O. (1978a) Structure of glasses and melts of $Na_2O\ xSiO_2$ ($x = 1, 2, 3$) composition from Raman spectroscopy. Carnegie Institution of Washington Year Book, 77, 649–652.

Sharma, S. K., Virgo, D. and Mysen, B. O. (1978b) Structure of melts along the join SiO_2–$NaAlSiO_4$. Carnegie Institution of Washington Year Book, 77, 652–658.

Shartsis, L., Spinner, S. and Capps, W. (1952) Density, expansivity and viscosity of molten alkali silicates. Journal of the American Ceramic Society, 35, 155–160.

Stewart, D. B. and Ribbe, P. H. (1969) Structural explanation for variations in all parameters of alkali feldspar with Al/Si ordering. American Journal of Science, 267A, 444–462.

Sweet, J. R. and White, W. B. (1969) Study of sodium silicate glasses and liquids by infrared spectroscopy. Physics and Chemistry of Glasses, 10, 246–251.

Taylor, M. and Brown, G. E. (1979a) Structure of mineral glasses. I. The feldspar glasses $NaAlSi_3O_8$, $KAlSi_3O_8$, $CaAl_2i_2O_8$. Geochimica et Cosmochimica Acta, 43, 61–77.

Taylor, M. and Brown, G. E. (1979b) Structure of mineral glasses. II. The SiO_2–$NaAlSiO_4$ join. Geochimica et Cosmochimica Acta, 43, 1467–1475.

Toop, G. W. and Samis, C. S. (1962) Activities of ions in silicate melts. Transactions of the Metallurgical Society AIME, 224, 878–887.

Verweij, H. (1979a) Raman study of the structure of alkali germanosilicate glasses. I. Sodium and potassium metagermanosilicate glasses. Journal of Non-Crystalline Solids, 33, 41–53.

Verweij, H. (1979b) Raman study of the structure of alkali germanosilicate glasses. II. Lithium, sodium and potassium digermanosilicate glasses. Journal of Non-Crystalline Solids, 33, 55–69.

Verweij, H. and Konijnendijk, W. L. (1976) Structural units in K_2O–PbO–SiO_2 glasses by Raman spectroscopy. Journal of the American Ceramic Society, 59, 517–521.

Virgo, D., Mysen, B. O. and Kushiro, I. (1980) Anionic constitution of silicate melts quenched at 1 atm from Raman spectroscopy: Implications for the structure of igneous melts. Science, 208, 1371–1373.

Virgo, D., Mysen, B. O., Danckwerth, P. and Seifert, F. A. (1982) Speciation of Fe^{3+} in 1-atm Na_2O–SiO_2–Fe–O melts. Carnegie Institution of Washington Year Book, 81, 349–352.

Virgo, D., Mysen, B. O. and Danckwerth, P. (1983) Redox equilibria and the anionic structure of $Na_2O \cdot xSiO_2$–Fe–O melts: Effect of oxygen fugacity. Carnegie Institution of Washington Year Book, 82, 305–309.

Visser, W. and Koster van Groos, A. F. (1979) Effect of P_2O_5 and TiO_2 on liquid-liquid equilibria in the system K_2O–FeO–Al_2O_3–SiO_2. American Journal of Science, 279, 970–988.

Wright, A. C., Rupert, J. P. and Granquist, W. T. (1968). High- and low-faujasites: a substantial series. American Mineralogist, 53, 1293–1303.

Manuscript received, October 21, 1983;
accepted for publication, August 21, 1984.